Structure and blood compatibility of highly oriented PLA/MWNTs composites produced by solid hot drawing

[1]Zhengqiu Li, [1]Xiaowen Zhao*, [1]Lin Ye, [2]Phil Coates, [2]Fin Caton-Rose, [2]Michasel Martyn

1. State Key Laboratory of Polymer Materials Engineering of China, Polymer Research Institute of Sichuan University, Chengdu, China

2. School of Engineering, Design and Technology, University of Bradford, Bradford, U.K.

*Corresponding author. Tel.: 862885408802; Fax: 862885402465. E-mail address: zhaoxiaowenscu@126.com

Abstract: Highly-oriented poly(lactic acid) (PLA)/multi-walled carbon nanotubes (MWNTs) composites were fabricated through solid hot drawing technology in an effort to improve the mechanical properties and blood biocompatibility of PLA as blood-contacting medical devices. It was found that proper MWNTs content and drawing orientation can improve the tensile strength and modulus of PLA dramatically. With the increase of draw ratio, the cold crystallization peak became smaller, and the glass transition and the melting peak of PLA moved to high temperature, while the crystallinity increased, and the grain size decreased, indicating of the stress-induced crystallization of PLA during drawing. MWNTs showed a nucleation effect on PLA, leading to the rise of the melting temperature, increase of crystallinity, and reduction of spherulite size for the composites. Moreover, the intensity of (002) diffraction of MWNTs increased with draw ratio, indicating that MWNTs were preferentially aligned and oriented during drawing. Microstructure observation demonstrated that PLA matrix had an ordered fibrillar bundle structure, and MWNTs in the composite tended to align parallel to the drawing direction. In addition, the dispersion of MWNTs in PLA was also improved by orientation. Introduction of MWNTs and drawing orientation could significantly enhance the blood compatibility of PLA by prolonging kinetic clotting time, reducing hemolysis ratio, and platelet activation.

Keywords: Poly (lactic acid) (PLA); multi-walled carbon nanotubes (MWNTs); composites; solid hot drawing; orientation; mechanical properties; blood compatibility

1. INTRODUCTION

Intense effort has been being made on preparing biomedical materials through centuries because of their extensive and significant importance in biology and medicine science [1]. Poly(lactic acid) (PLA) has been considered to be a good candidate for biomedical materials due to its favorable physical properties, ease of handling and processing, and its biodegradable and biocompatible nature, which have been approved by the Food and Drug Administration (FDA) for numerous clinical applications, such as sutures, bone plates, abdominal mesh, and extended-release pharmaceuticals [2~4].

For biomedical materials, two fundamental requirements are proposed. First, their physical properties such as flexibility or rigidity, mechanical strength, etc., must fulfill the purposes for multiple practices relating with biological preference. In addition, it is evident that, for any clinical application, biocompatibility which consists of both blood biocompatibility and tissue biocompatibility of the material is crucial. And for a biomedical implant material to be in contact with blood, the blood compatibility is proved one of the most important properties to ensure the security of clinical practice [5~6].

Although extensive efforts have been devoted to modifying the mechanical properties of PLA by copolymerization with other monomers or blending PLA with other polymers, limited studies have been reported on the blood compatibility of PLA [7~9].

Molecular orientation in polymers greatly improves their mechanical and physical properties compared to isotropic materials. Solid phase hot drawing is one of the methods of molecular orientation in the solid state of polymers. In this process, polymers are processed below the crystalline melting temperature in the case of semicrystalline polymer or near the glass transition temperature for amorphous polymer, and high production rates and high orientation can be achieved without complex processing apparatus, and thick section samples, including tubes, tapes, etc., can be produced[10-12]. Through solid hot drawing technology,

first of all, PLA with sufficient initial strength and sufficient strength retention over a period of time could be prepared to meet the requirement of desirable physical properties for biomedical use. Meanwhile, the surface properties of PLA may be influenced by processing and thus affect the interaction with the biological elements of the organism. Grijpma et al[13] reported that oriented poly (D,L-lactide) could be obtained by drawing injection moulded specimens at temperatures below the glass transition temperature of the polymer. High mechanical properties, with tensile strength of 73 MPa and elongation at break of 48% were achieved. Yang et al[14] reported the preparation of orientation-structured microtubules of PLA by phase separation of the polymer solution through the process of cooling and freeze-drying. Wong et al [15] described uni-axial sample drawing of PLA carried out on a universal Instron testing machine. However, the stretch ratio was as low as 2~4 due to the brittle tensile behavior of PLA and the effect of orientation on the blood compatibility of PLA has not been studied.

Carbon materials are known to be inert to cells and tissues because of their pure carbon compositions. Carbon nanotubes (CNTs), rolled graphite sheets with nanoscale diameters, have attracted a significant attention due to their unique properties, such as high hardness, low coefficient of friction, chemical inertness, high wear and corrosion resistance, which make CNTs excellent candidates for manufacturing biocompatible polymer composites [16~19].

In this work, PLA was mixed with the hydroxylated MWNTs, and the highly oriented PLA and PLA/MWNTs composites were first successfully fabricated through solid hot drawing technology. Take advantage of one-dimensional (1D) nanostructures of MWNTs to form joint orientation with PLA matrix during processing for further improving the mechanical properties and blood biocompatibility of PLA as blood-contacting medical devices. The structure and properties of the oriented composites were studied.

2. EXPERIMENTAL SECTION

2.1 Materials

Poly(L-lactic acid) (PLA) used in this study was a commercial grade granular product without any additives (Cargill Dow Co., USA). The molecular weight ($\overline{M_n}$) was about 1 × 10^5g mol^{-1}. Multi-walled carbon nanotubes (MWNTs) with about 1.63wt% hydroxyl group and a small amount of carboxyl groups were supplied by Chengdu Institute of Organic Chemistry (Chengdu, China), and synthesized from natural gas via catalytic chemical vapor deposition, with average length of 10~30μm, diameter of 20~40 nm.

2.2 Preparation of the oriented PLA/MWNTs composites

Preparation of PLA/MWNTs composites

The granules of PLA and MWNTs were compounded and extruded by a TSSJ-25/03 twin-screw extruder (Chenguang Chemical Engineering Research Institute, China) at a rotational speed of 45 rpm, and the temperature of the barrel was in the range of 180 ^{o}C ~to 220 ^{o}C. The extrudate was pelletized and dried, and then moulded to tensile specimens according to ISO 527-1-2012(E) by using K-TEC40 injection moulding machine (Ferromatik Milacron Ltd., Germany). The barrel temperature profile was 160°C (hopper)~190°C (nozzle) and the mould temperature was maintained at 50°C.

Preparation of the oriented PLA/MWNTs composites

The oriented samples of PLA and PLA/MWNTs composites were prepared by being heated at 90 ^{o}C and mechanically stretched through a converging die with drawing rate of 25mm/min. The draw ratio (DR) of the sample was determined with the following equation:

$$DR = 100\ \%*(S - S_0)/S_0 \qquad (1)$$

where S_0 is the cross-sectional area prior to drawing and S is the final cross-sectional area after drawing.

After the desired draw ratio was obtained, the sample was cooled down to room temperature, and then the load was released.

2.3 Measurements

Mechanical properties

The mechanical properties of PLA samples were measured by Instron 4302 material testing machine (Instron Co., USA) according to ISO 527-1-2012(E). The test speed was 50 mm/min, and the sample length between benchmarks was 25 mm. All the values presented were the average of five specimens.

Non-isothermal crystallization analysis

The non-isothermal crystallization was performed with a Netzsch 204 Phoenix differential scanning calorimetry (DSC) (Netzsch Ltd., Germany). The temperature scale of DSC was calibrated with indium. Granulated samples of about 10 mg were heated from ambient temperature to 200^{o}C at a constant rate of 10 K/min under nitrogen atmosphere. X_c can be calculated with the following equation:

$$X_c=100\%*(\Delta H_m/\Delta H_0) \qquad (2)$$

where ΔH_m and ΔH_0 are the melting enthalpies for the samples and the 100% crystalline PLA, respectively. The melting enthalpy of a totally crystalline PLA material (ΔH_0) was considered to be 93 J/g [20]. An overall accuracy of ±0.5 °C in temperature and ±1% in enthalpy was estimated.

Wide-angle X-ray diffraction analysis (WAXD)

WAXD analysis was performed with a Rigaku D/max IIIB X-ray diffractometer (Rigaku Co., Japan) at room temperature. WAXD data were collected from 5 to 35^{o}.

The crystallinity of PLA can be calculated by the peak area of crystal and amorphous region form WAXD curves using PeakFit software (version 1.00, Jandel Scientific, San Rafael, CA)

When the grain size is below 10μm, the polycrystal X-ray diffraction peak broaden remarkably. Based on the widen amount of diffraction peak, the grain size can be calculated with the following equation:

$$L_{hkl} = \frac{k\lambda}{\beta \cos\theta} \quad (3)$$

Where L_{hkl} is the grain size of normal direction of (hkl) crystal plane; θ is the Bragg angle; β is the widening amount of diffraction peak attributed to the decrease of the grain size; λ is the wave length of entrance X-ray; k is a constant.

Molecular weight measurement

The molecular weight distribution and relative molecular weight of PLA before and after solid hot drawing were determined by gel permeation chromatography (GPC). PLA specimens were dissolved in tetrahydrofuran (THF) at a concentration of 5 mg/mL and 10 μL of the test solution was injected in a GPC apparatus (Shimadzu Co., Kyoto, Japan) equipped with two GPC columns (Super HM-H (6.0mm*15cm*2)，Tokyo, Japan), a refractive index detector (model RI, Shimadzu Co.) and Class-LC workstation GPC software (Shimadzu Co.). The flow rate of chloroform mobile phase was 0.6 ml/min. Molecular weight values, including weight average ($\overline{M_w}$), number average ($\overline{M_n}$), and molecular weight distribution ($\overline{M_w / M_n}$) for PLA were measured from the comparison with the calibration line which was made with polystyrene standards (Showa Denko, Tokyo, Japan).

Scanning electron microscope analysis

The fractured surface morphology analysis of the samples was performed with JSM-5900LV scanning electron microscope (JEOL Ltd.，Japan) with an acceleration voltage of 20 kV. The samples were sputter-coated with gold for 2~3 min.

Contact angle measurement

The contact angles of deionized water and glycerol (AR, Ke Long Co., China)as testing liquids on the samples were measured by an ErmaG-1 contact angle test apparatus (Shimadzu Co., Japan) at room temperature using the sessile drop method. Five measurements were made on each sample to obtain the values of contact angle.

Hemolysis analysis

Hemolytic activity was assessed by determining hemoglobin release under static conditions using the two phase hemolysis test (according to ASTM F 756-00). Blood testing solution was prepared by using 4 mL fresh blood with an acid citrate dextrose anticoagulant (ACD medium) and was diluted with 5 mL of physiological saline. In the first phase, each sample (1 cm × 1 cm) was incubated in 10 mL pure physiological saline for 30 min at 37 ^{o}C. Then, diluted fresh blood (0.2 mL) was added and incubation went on for another 60 min in a shaker at the constant temperature of 37 ^{o}C. Positive and negative controls were produced by adding 0.2 mL of diluted fresh blood to 10 mL of purified water and saline, respectively. After incubation, samples were centrifuged at 2500 r/min for 5 min. Optical density (O.D) of the supernatant was measured at 545 nm by an U3010 UV-visible spectrophotometer (Shimadzu Co., Japan). The hemolysis ratio was calculated according to Equation 4 and all the values presented were the average of three specimens.

$$Z=100\%*(D_t-D_{nc})/(D_{pc}-D_{nc}) \qquad (4)$$

Where Z represented the hemolysis ratio, D_t represented the absorptance of test samples, D_{nc} and D_{pc} represented the negative samples and positive samples, respectively (ASTM F 756-00).

Kinetic clotting time

Kinetic clotting time was measured as follows: 100 μL of anticoagulant blood was carefully added on the surface of test samples (1 cm × 1 cm), followed by the addition of 10

μL of calcium chloride solution (0.2 mol/L) simultaneously. Thereafter, time was recorded. After the preset, 10, 20 30, 40 and 50 min, the surface of the test sample with blood was rinsed slowly by the distilled water separately and the rinsed liquid was collected. Then the optical density (O.D) of this collected liquid was measured with an U3010 UV–visible spectrophotometer (Shimadzu Co., Japan) at a wavelength of 545 nm. Glass silicide and glass were used as a negative control and a positive control, respectively. All the values presented were the average of three specimens.

Platelet adhesion measurement

To test the platelet adhesion, the specimens in square shape (1cm×1cm) were incubated with the platelet rich plasma (PRP) for 1 h at 37^{o}C under static conditions. After 1 h incubation, the samples were rinsed carefully three times with phosphate-buffered saline buffer (PBS, 0.01M sodium phosphate buffer, 150mM NaCl, pH=7.4). The adherent platelets were fixed using 2.5% glutaraldehyde in PBS for at least 1 h, dehydrated in a graded series (50%, 60%, 70%, 80%, 90%, 95%, and 100%, v/v) of ethanol, and dried under vacuum at -50^{o}C overnight. The samples were then sputter coated with a thin layer of gold and observed using a JSM-5900LV scanning electron microscopy (JEOL Ltd., Japan).

3. RESULTS AND DISCUSSION

3.1 Mechanical properties of drawn PLA/MWNTs composites

The mechanical properties of isotropic and drawn PLA/MWNTs composites in comparison with neat PLA were shown in Figure 1. Compared to the neat PLA, the addition of the MWNTs brought about some increase in tensile strength and modulus, which could be attributed to the reinforcement of the rigid MWNTs. With the increase of MWNTs content, the tensile strength and modulus of the composites initially increased, and then declined slightly above 10wt% of MWNTs which may caused by the poor dispersion and aggregation

of MWNTs in PLA matrix at high MWNTs content. The elongation at break of the composites showed a downward trend with increasing MWNTs content.

With increasing draw ratio, the tensile strength and modulus increased sharply, while the elongation at break decreased for both PLA and PLA/MWNTs composites. At the same draw ratio, the tensile strength and modulus of the PLA/MWNTs composites were higher than that of the neat PLA, while the elongation at break was lower than PLA. At 480% of draw ratio, the tensile strength of the PLA/5wt% MWNTs composites can reach up to 233 MPa, and the tensile modulus was 9.9GPa. The mechanical properties were much higher than the values previously reported for oriented PLA [21].

After drawing, the stress increased dramatically in a low-strain region on the stress-strain curves of PLA and PLA/5wt% MWNTs composites, and the high modulus can be achieved. Different from isotropic PLA and the general semi-crystalline polymers, no necking was observed, and a uniform deformation occurred for the samples oriented. Moreover, the area surrounded by the stress-strain curve was reduced with the increase of draw ratio, indicating that the stiffness and brittleness increased.

3.2 Structure and morphology of drawn PLA/MWNTs composites

3.2.1 Crystallization property

DSC measurements were performed in order to evaluate the influence of processing conditions on the crystallization properties of PLA and PLA/MWNTs composites. The DSC thermograms of isotropic and drawn samples were shown in Figure 2, from which the melting temperature (T_m), the heat of melting (ΔH_m) and the crystallinity (X_c) can be obtained, as listed in Table 1.

All samples exhibited three distinct peaks corresponding to glass transition at around 60 °C, cold crystallization peaks at about 80 °C, and melting peaks at around 170 °C respectively. Compared with the neat PLA, the cold crystallization peak became smaller,

while the glass transition and the melting peak moved to high temperature for PLA/MWNTs composites.

With increasing the draw ratio, the melting peaks and the glass transition of PLA and PLA/MWNTs composites gradually moved to high temperature, moreover, the cold crystallization peaks became smaller and even disappeared at high draw ratio.

As shown in Table 1, the melting enthalpy and crystallinity of PLA increased with the draw ratio, indicating of the stress-induced crystallization of PLA during drawing. At the same draw ratio, the melting enthalpy and crystallinity of PLA increased with the increase of MWNTs content, which demonstrated the nucleation effect of MWNTs on PLA. Due to the large aspect ratio, high specific surface area and strong interfacial interaction of –OH and –COOH on MWNTs with PLA matrix [22], the PLA molecules can easily be bounded on the surface of MWNTs, which can form a sufficient number of nucleation centers and play the role of crystal nucleus.

Wide-angle X-ray diffraction (WAXD) measurements were taken to further confirm the crystallization behavior of PLA and PLA/MWNTs composites during solid hot drawing technology. Figure 3 displayed the WAXD patterns in the range of $2\theta=5\sim35^{o}$ for the neat PLA and the PLA/MWNTs composites. The samples before drawing exhibited a diffraction peak at $2\theta = 16.7°$, which belonged to α crystal form of PLA as reported previously [23]. It can be seen that the diffraction peak position of oriented PLA and PLA/MWNTs composites with different draw ratio had no change, however, there were significant differences in intensity. Because the intensity of the diffraction peak represented the degree of the order in the material, including crystallization and orientation, the results indicated that drawing did not affect the crystal type, but it could significantly affect the crystallization and orientation of PLA.

Compared to neat PLA, in addition to the diffraction peak attributed to PLA, the patterns of the PLA/MWNTs composites presented a new diffraction peak around 26.1^{o} in 2θ, corresponding to a d-spacing of 3.4 Å, which was the intershell spacing within the nanotubes. For the composites before drawing, when the MWNTs were randomly dispersed inside the polymer matrix, a relative low intensity distribution was expected. With increasing draw ratio, the diffraction intensities of the MWNTs increased, suggesting that MWNTs were preferentially oriented along the draw direction.

The crystallinity of PLA and PLA/MWNTs can be calculated by PeakFit software and the calculated data were summarized in Table 2. The grain sizes of samples calculated according to Equation (3) were also listed in Table 2.

As shown in Table 2, with the increase of the draw ratio, the crystallinity of PLA increased, while the grain size of PLA decreased, indicating that slipping and rupture of the lamellar in the spherulite occurred during the drawing of PLA and a clear orientation of PLA molecules formed. Compared with the neat PLA at the same draw ratio, the crystallinity of PLA in the composites was higher and the grain size of PLA was lower, indicating that the interaction between PLA and MWNTs promoted the crystallization of PLA molecules during drawing. The trend of crystallinity obtained from WAXD was highly reproducible and consistent with DSC results and the values were close to that of oriented PLA reported in the literature [24].

3.2.2 Molecular weight analysis

The molecular weight ($\overline{M_w}$ and $\overline{M_n}$) and molecular weight distribution ($\overline{M_w / M_n}$) of PLA before and after solid phase drawing determined by GPC were shown in Table 3. Samples after oriented processing showed slightly decrease in molecular weight and the $\overline{M_w / M_n}$ value remained unchanged during processing indicating that no severe degradation

occurred during the solid hot drawing process.

3.2.3 Orientation morphology

The section morphology of PLA and PLA/MWNTs composites drawn at different draw ratios was shown in Figure 4. It can be seen that the sections of all samples with different draw ratios exhibited orderly arranged fibrillar bundle structure as shown in Figure 4(a~d, e~g, i~j), and these micro-fibers were mainly composed of highly oriented folded lamellar crystals of PLA and noncrystal parts oriented along the drawing direction which alternately and periodically arranged [25]. The fibrillar bundle structure had also been observed for PLA spinning fiber [26]. The formation of these high oriented micro-fibers contributed to the significantly high tensile strength and modulus of the samples.

The section morphology of PLA/5wt%MWNTs composites drawn at different draw ratios was shown in Figure 4(e-h). After drawing, highly oriented micro-fibers of PLA matrix can be found. And at the same time, from the high magnified images (Figure 4(h)), the alignment of MWNTs along with the draw direction can also be observed.

When employing with a content of 15wt%, a notable orientation for both PLA and MWNTs can be observed from the section morphology of the composites (Figure 4(i~j)). Moreover, excessive addition of MWNTs led to the poor dispersion and aggregation of MWNT in PLA matrix as shown in the highlight region of high magnified images (Figure 4(k)). The dispersion of MWNTs in PLA can be improved by orientation, as shown in Figure 4(l).

3.3 Contact angle of drawn PLA/MWNTs composites

Surface properties such as availability of certain functional groups, domain structure, electrical charge, hydrophilicity/hydrophobicity, interfacial adaptability and surface roughness are considered to determine the fate of blood proteins, enzymes and cells interacting with the materials which, in turn, can induce several cascade reactions and activation phenomena

[27].In particular, the surface wettability is expected to play a significant role in terms of blood compatibility.

Water and glycerol contact angles of the PLA and PLA/MWNTs composites as determined by the sessile drop method were listed in Table 4. All PLA/MWNTs composites had lower water contact angle than neat PLA at the same draw ratio, perhaps due to hydrophilicity of the –OH and –COOH groups on the surface of MWNTs, while the water contact angle also decreased with the increase of draw ratio for both PLA and PLA/MWNTs composites. The contact angle with glycerol fluctuated for different samples. The above result indicated that the surface properties of PLA were significantly influenced by the introduction of MWNTs and the alignment of PLA and MWNTs. Therefore, for drawn PLA and PLA/MWNTs composites, it was thought that the different blood compatibility may be due to their different surface properties.

3.4 Blood compatibility of drawn PLA/MWNTs composites

3.4.1 Hemolysis ratio

Hemolysis of the blood is an extremely serious problem associated with the non-biocompatibility of materials faced by biomaterial researchers. Red blood cells may hemolyze when contacting with implant materials and thus cause eventually failure [28~29]. Therefore, in evaluating blood compatibility and biocompatibility, it is of vital importance to investigate the hemolysis ratio of the material. Here, PLA and PLA/MWNTs composites at different drawing stages were selectively chosen to explore their hemolytic activity.

Results obtained from hemolysis test of ACD blood for PLA and PLA/MWNTs composites were shown in Table 5. According to the related standard (ASTM F 756-00), permissible hemolysis ratio of biomaterials should be at least lower than 5%. Therefore, first, the hemolysis ratio of 2.84% for neat PLA makes it suitable as the substrate material. As to the surface of PLA/MWNTs composites before drawing, an obviously less hemolysis rate was

obtained indicating that the MWNTs would improve the compatibility of the composites to a certain extent when contacting with biofluids. More importantly and promisingly, a key finding here was the fact that the surface of the sample after drawing with different draw ratio was much less hemolytic than the isotropic one. Therefore, leading to less damage of red blood cells, the oriented PLA and oriented PLA/MWNTs composites exhibited desirable blood compatibility.

3.4.2 Kinetic clotting time

Figure 5 showed the curves of optical density (O.D) value versus time for the PLA and PLA/MWNTs composites with different draw ratio. The clotting time measurement was to test the activated degree of intrinsic coagulation factors. The higher absorbance, the better thrombo resistance was. A similar change tendency of the O.D value for all samples was observed: decreasing with the increase of the contact time. Compared with neat PLA, PLA/MWNTs composites had higher absorbance at the same clotting time, indicating that the composites possessed better blood compatibility than neat PLA. Moreover, the clotting trend of the drawn sample was much lower than that of the sample before drawing, which indicated that the blood compatibility of the PLA and PLA/MWNTs composites was improved by orientation.

Generally, the time when O.D value is equal to 0.1 is defined as initial clotting time. From Figure 5, it can be seen that, the initial clotting time of the oriented samples was longer than that of isotropic samples, and compared with neat PLA before drawing, the initial clotting time of PLA/5%MWNTs composites with draw ratio of 480% increased by almost 37min.

3.4.3 Platelet adhesion

When platelets are activated, they will deform and crosslink to promote aggregation of further platelets. Platelet adhesion and activation on the surface of a biomaterial is the most

essential character in determining the blood compatibility of a biomaterial [30]. Low platelet adhesion and activation denotes good blood compatibility, while a higher degree of platelet adhesion and activation could result in a thrombus.

The platelet adhesion densities on the polymers were evaluated, as shown in Figure 6. After contact with PRP for 60 min, a large number of platelets were observed to aggregate on the surface of isotropic PLA samples, however, the platelet adherent density on the oriented PLA with different draw ratio was significantly lower than that on PLA before drawing. Although the number of platelets on oriented PLA became fewer, there was still a certain degree of activation.

In the case of PLA/MWNTs composites, however, the surface seemed prone to prevent platelets from adhering, since much fewer platelets were observed, especially in the case of PLA/5%MWNTs with draw ratio of 480%, indicating that the activation of platelets on PLA/MWNTs composites was limited.

4. CONCLUSIONS

Highly-oriented PLA/MWNTs composites with enhanced mechanical properties and good blood compatibility were fabricated through solid hot drawing technology. The tensile strength and modulus of the composites increased significantly by drawing for both PLA and PLA/MWNTs composites. By using suitable content of MWNTs, the mechanical strength of the composites can also be improved. With the increase of draw ratio, the cold crystallization peak became smaller, and the glass transition and the melting peak moved to high temperature, while the crystallinity increased, and the grain size of PLA decreased, indicating of the stress-induced crystallization during drawing. MWNTs showed the nucleation effect on PLA, leading to the rise of the melting temperature, increase of crystallinity and reduction of spherulite size for the composites. With the increase of draw ratio, the intensity of (002) diffraction of MWNTs increased indicating that MWNTs in composites were aligned and

oriented during drawing. The section of all drawn PLA and PLA/MWNTs composites exhibited orderly arranged fibrillar bundle structure, and for the composites, MWNTs tended to align parallel to the drawing direction. The dispersion of MWNTs in PLA can be improved by orientation at high MWNTs content. Results obtained from hemolysis test showed that, before drawing, an obviously less hemolysis rate than neat PLA was obtained for the composites, and after drawing, the oriented surface was much less hemolytic than the isotropic one. The clotting trend of the drawn sample was much lower than that of the sample before drawing, and compared with neat PLA, PLA/MWNTs composites had higher absorbance at the same clotting time, indicating that the composites possessed better blood compatibility. After contacting with the PRP for 60 min, the platelet adherent density on oriented PLA was significantly lower than that on PLA before drawing. In the case of PLA/MWNTs composites, much less platelets were observed, especially in the case of PLA/5% MWNTs with draw ratio of 480%, indicating that the activation of platelets on PLA/ MWNTs composites was limited. The conclusion mentioned may lay a foundation for the research and development of new types of PLA blood compatible materials and its application as biomedical materials.

ACKNOWLEDGEMENTS

This work was supported by Science Bridges China Project.

References

[1] Tsuruta, T. Contemporary Topics in Polymeric Materials for Biomedical Applications, *Adv. Polym. Sci.*, 1996: **126**: 1-51.

[2] Okada, H., Heya, T., Igari, Y., Ogawa, Y., Toguchi, H. and Shimamoto, T. One Month Release Injectable Microspheres of Leuprolide Acetate Inhibit Steroidogenesis and Genital Organ Growth in Rats, *Int. J. Pharm.*, 1989: **54**: 231-239.

[3] Kapadia, C., Mann, J., McGeehan, D., Biglin, J. and Waxman, B. Behavoir of Synthetic Absorbable Sutures with and without Synergistic Enteric Infection, *Eur. Surg. Res.*, 1983: **15**: 67-72.

[4] Debus, E., Geiger, D., Sailer, D., Ederer, J. and Theide, A. Physical, Biological and Handling Characteristics of Surgical Suture Material, *Eur. Surg. Res.*, 1997: **29**: 52-61.

[5] Banerjee, B., Nageswari, K., Puniyani, R. R. Hematological Aspects of Biocompatibility, *Journal of Biomaterials Applications*, 1997: **12**: 57-76.

[6] Wen, X.W., Pei, S.P., Li, H., Ai, F., Chen, H., Li, K.Y., Wang, Q. and Zhang, Y.M. Study on an Antifouling and Blood Compatible Poly(ethylene–vinyl acetate) Material with Fluorinated Surface Structure, *J. Mater. Sci.*, 2010: **45**: 2788–2797.

[7] Nagahama, K., Ohya, Y. and Ouchi, T. Synthesis of Star-Shaped Arms Poly(ethylene glycol)-Poly(L-lacitde) Block Copolymer and Physical Properties of Its Solution Cast Film as Soft Biomaterial, *Polym. J.*, 2006: **38**: 852-860.

[8] Helminen, A.O., Korhonen, H. and Seppala, J.V. Cross-Linked Poly-(ε-caprolactone/D,L-lactide) Copolymers with Elastic Properties, *Macromol. Chem. Phys.*, 2002: **203**: 2630-2639.

[9] Nijenhuis, A.J., Colstee, E., Grijpma, D.W. and Pennings, A.J. High Molecular Weight Poly(l-lactide) and Poly(ethylene oxide) Blends: Thermal Characterization and Physical Properties, *Polymer*, 1996: **37**: 5849-5857.

[10] Stell, J.R., Paul, D.R., Barlow J.W. Mechanical properties of oriented polyethylene/ polystyrene blends, *Polymer Engineering & Science*, 1976: **16**: 496–506

[11] McCullough, R.D. Tristram-Nagle, S. Self-orienting head-to-tail poly (3-alkylthiophen

es): new insights on structure-property relationships in conducting polymers, *JACS*, 1993: **115**: 4910–4911

[12] Majola, A., Vainionpää, S., Rokkanen, P., Mikkola, H.M., Törmälä P. Absorbable self-reinforced polylactide (SR-PLA) composite rods for fracture fixation: strength and strength retention in the bone and subcutaneous tissue of rabbits, *Journal of Materials Science: Materials in Medicine*, 1992: **3**: 43-47

[13] Grijpma, D. W., Altpeter, H., Bevis, M. J., Feijen, J. Improvement of the mechanical properties of poly(D,L-lactide) by orientation, *Polymer International*, 2002: **51**: 845-851

[14] Yang, F., Qu, X., Cui, W., Bei, J., Yu, F., Lu, S., Wang, S. Manufacturing and morphology structure of polylactide-type microtubules orientation structured scaffolds, *Biomaterials*, 2006: **27**: 4923 – 4933

[15] Wong, S., Wu, J. S., Leng, Y. Mechanical Behavior of PLA/HA Composite in Simulated Physiological Environment, *Key Engineering Materials*, 2005: **288-289**: 231-236

[16] Miguel, A., Correa D., Nicholas, W. and Chapana, J.R. Fabrication and Biocompatibility of Carbon Nanotube-Based 3D Networks as Scaffolds for Cell Seeding and Growth, *Nano Letters*, 2004: **11**: 2233-2236.

[17] Zhang, D.H., Madhuvanthi, A., Kandadai, Cech, J., Siegmar R. and Seamus, A. Poly(L-lactide) (PLLA)/Multiwalled Carbon Nanotube (MWCNT) Composites: Characterization and Biocompatibility Evaluation, *J. Phys. Chem. B.*, 2006: **110**:

12910-12915.

[18] Katsumune, T., Rumi, S., Uchida, K. and Hirofumi, Y. Improved Blood Biocompatibility of Composite Film of Chitosan/Carbon Nanotubes Complex, *J. Biorheol.*, 2009: **23**: 64–71.

[19] Ko, S.W., Hong, M.K., Park, B.J., Gupta, R.K., Choi, H.J. and Bhattacharya, S.N. Morphological and Rheological Characterization of Multi-walled Carbon Nanotube-/PLA/PBAT Blend Nanocomposites, *Polym. Bull.*, 2009: **63**: 125–134.

[20] Liu, X., Dever, M., Fair, N., Benson, R. S. Thermal and mechanical properties of poly (lactic acid) and poly (ethylene/butylene succinate) blends, *Journal of environmental polymer degradation*, 1997: **5**: 225-235

[21] Stoclet, G., Seguela, R., Lefebvre, J. M., Elkoun, S. Strain-induced molecular ordering in polylactide upon uniaxial drawing, *Macromolecules*, 2010: **43**: 1488–1498

[22] Yoon, J.T., Jeong, Y.G., Lee, S.C. Influences of poly(lactic acid)-grafted carbon nanotube on thermal, mechanical, and electrical properties of poly(lactic acid), *Polym. Adv. Technol.*, 2009: **20**: 631–638.

[23] Marubayashi, H., Asai, S. Sumita M. Complex Crystal Formation of Poly(l-lactide) with Solvent Molecules, *Macromolecules*, 2012: **45**: 1384–1397.

[24] Fei, F., Lin, Y. Morphologies and mechanical properties of polylactide/thermoplastic polyurethane elastomer blends, *Journal of Applied Polymer Science*, 2011: **119**: 2778–2783

[25] Peek, G.J. and Firmin, R.K. The Inflammatory and Coagulative Response to Prolonged

Extracorporeal Membrane Oxygenation, *ASAIO J.*, 1999: **45**: 250-263.

[26] Dersch, R., Liu, T., Schaper, A. K., Greiner, A., Wendorff, J. F. Electrospun nanofibers: Internal structure and intrinsic orientation, *Journal of Polymer Science Part A: Polymer Chemistry*, 2003: **41**: 545–553

[27] Ratner, B.D. The Catastrophe Revisited: Blood Compatibility in the 21st Century, *Biomaterials*, 2008: **28**: 5144-5147.

[28] Xiong, L., He, Z. The biological evaluation of the PEG/PLA amphiphilic diblock copolymer, *Plastics Technology and Engineering*, 2010: **12**: 1201-1206.

[29] Shen, F., Zhang, E., Wei, Z. In vitro blood compatibility of poly (hydroxybutyrate-co-hydroxyhexanoate) and the influence of surface modification by alkali treatment, *Materials Science and Engineering: C*, 2010: **30**: 369-375.

[30] Courtney, J. M.,Lamba, N. M. K.,Sundaram, S., Forbes, C. D. Biomaterials for blood-contacting applications, *Biomaterials*, 1994: **15**: 737-744

Table caption

Table 1 DSC parameters of oriented PLA and PLA/MWNTs composites

Table 2 Crystallinity and grain size of oriented PLA and PLA/MWNTs composites obtained by WAXD

Table 3 Molecular weight of PLA before and after drawing

Table 4 Contact angles of oriented PLA and PLA/MWNTs composites

Table 5 Hemolytic activity of oriented PLA and PLA/MWNTs composites

Table 1 DSC parameters of oriented PLA and PLA/MWNTs composites

Sample	Draw ratio (%)	T_m（^oC)	△H（J/g)	X_c（%)
PLA	0	168.5	25.74	27.7
	280	169.2	27.96	30.1
	340	170.6	30.9	33.3
	480	170.9	32.57	35.1
PLA/5wt%MWNTs	0	169.2	26.74	28.6
	280	169.7	27.33	29.4
	340	170.1	30.4	32.5
	480	170.2	32.77	35.1
PLA/10wt%MWNTs	0	169.3	26.34	28.1
	280	169.9	27.55	29.5
	340	170.8	30.67	32.8
PLA/15wt%MWNTs	0	170.3	26.98	28.9
	280	171.1	28.32	30.5

Table 2 Crystallinity and grain size of oriented PLA and PLA/MWNTs composites obtained by WAXD

Samples	Draw ratio（%）	Crystallinity（%）	Grain size（Å）
PLA	0	30.2	284
	280	38.9	164
	340	41.2	92
	480	44.3	65
PLA/5wt%MWNTs	0	33.2	212
	280	40.7	155
	340	45.5	103
	480	50.3	89
PLA/10wt%MWNTs	0	30.2	205
	280	38.7	163
	340	42.1	114
PLA/15wt%MWNTs	0	30.4	166
	280	37.2	167

Table 3 Molecular weight of PLA before and after drawing

Samples	$\overline{M_n}$ ($\times 10^4$ g mol^{-1})	$\overline{M_w}$ ($\times 10^4$ g mol^{-1})	$\overline{M_w}/\overline{M_n}$
PLA before drawing	5.78	11.60	2.01
PLA after drawing	5.69	11.44	2.01

Table 4 Contact angles of oriented PLA and PLA/MWNTs composites

Samples	Draw ratio(%)	Contact angle(^{o})	
		Water	Glycerol
PLA	0	74	65
	280	63	61
	340	65	64
	480	69	65
PLA/5wt%MWNTs	0	70	58
	280	64	64
	340	64	61
	480	52	67
PLA/10wt%MWNTs	0	70	62
	280	65	63
	340	61	60
PLA/15wt%MWNTs	0	69	52
	280	59	58

Table 5 Hemolytic activity of oriented PLA and PLA/MWNTs composites

Samples	Draw ratio(%)	Hematolysis rate（%）
PLA	0	2.84
	280	0.00
	340	0.22
	480	0.00
PLA/5wt%MWNTs	0	1.36
	280	0.53
	340	0.43
	480	0.00
PLA/10wt%MWNTs	0	3.18
	280	2.72
	340	0.45
PLA/15wt%MWNTs	0	1. 59
	280	1. 36

Figure caption

Figure 1 Mechanical properties of oriented PLA and PLA/MWNTs composites

Figure 2 DSC curves of oriented PLA and PLA/MWNTs composites

Figure 3 WAXD curves of oriented PLA and PLA/MWNTs composites

Figure 4 SEM images of oriented PLA and PLA/MWNTs composites

Figure 5 Curves of kinetic clotting time of oriented PLA and PLA/MWNTs composites

Figure 6 Platelet adsorption of oriented PLA and PLA/MWNTs composites（Magnification: 5000×）

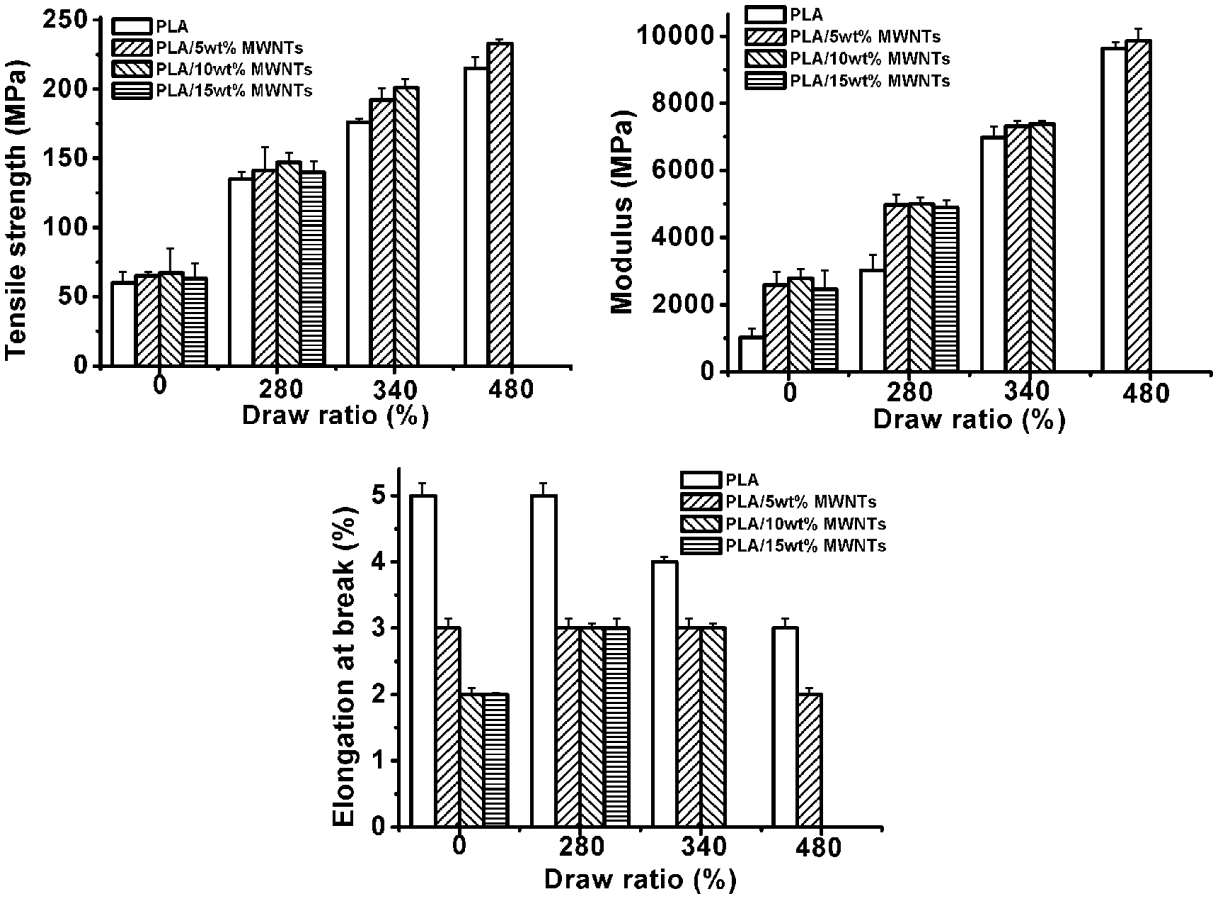

Figure 1 Mechanical properties of oriented PLA and PLA/MWNTs composites

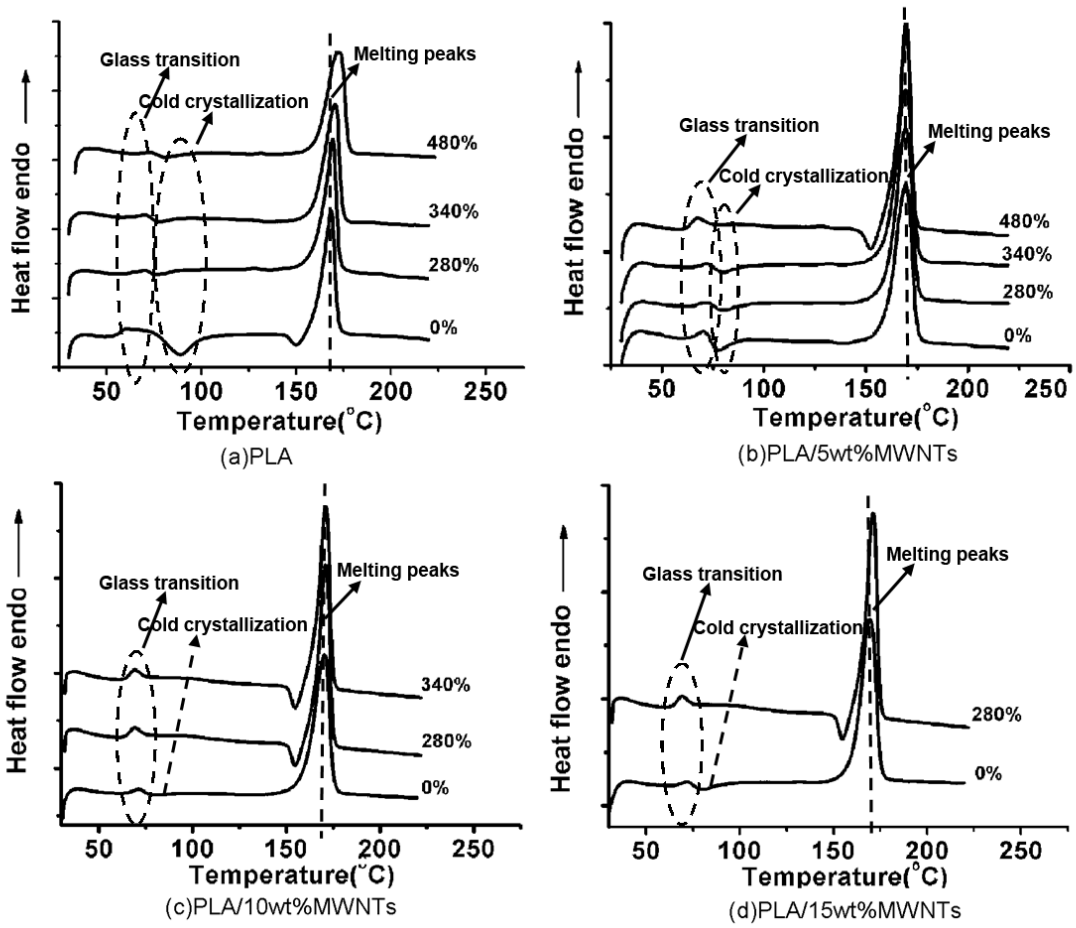

Figure 2 DSC curves of oriented PLA and PLA/MWNTs composites

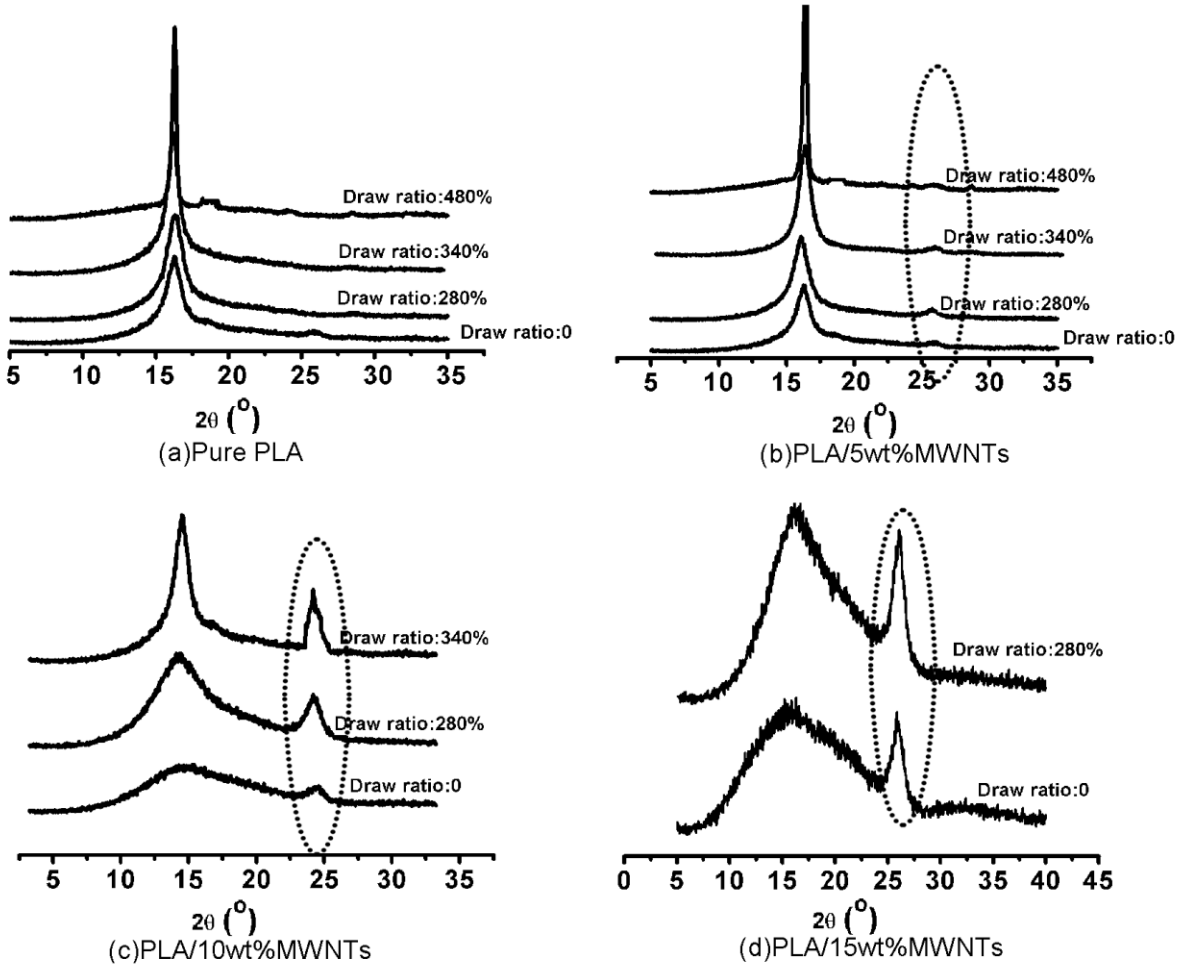

Figure 3 WAXD curves of oriented PLA and PLA/MWNTs composites

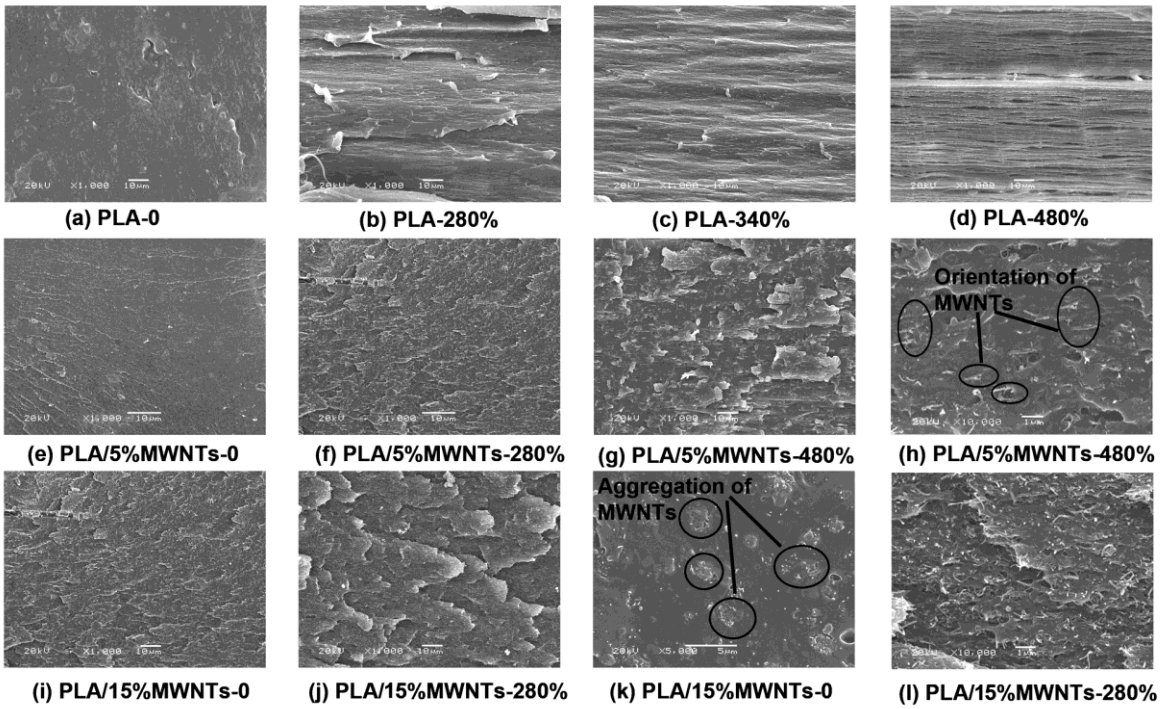

Figure 4 SEM images of oriented PLA and PLA/MWNTs composites

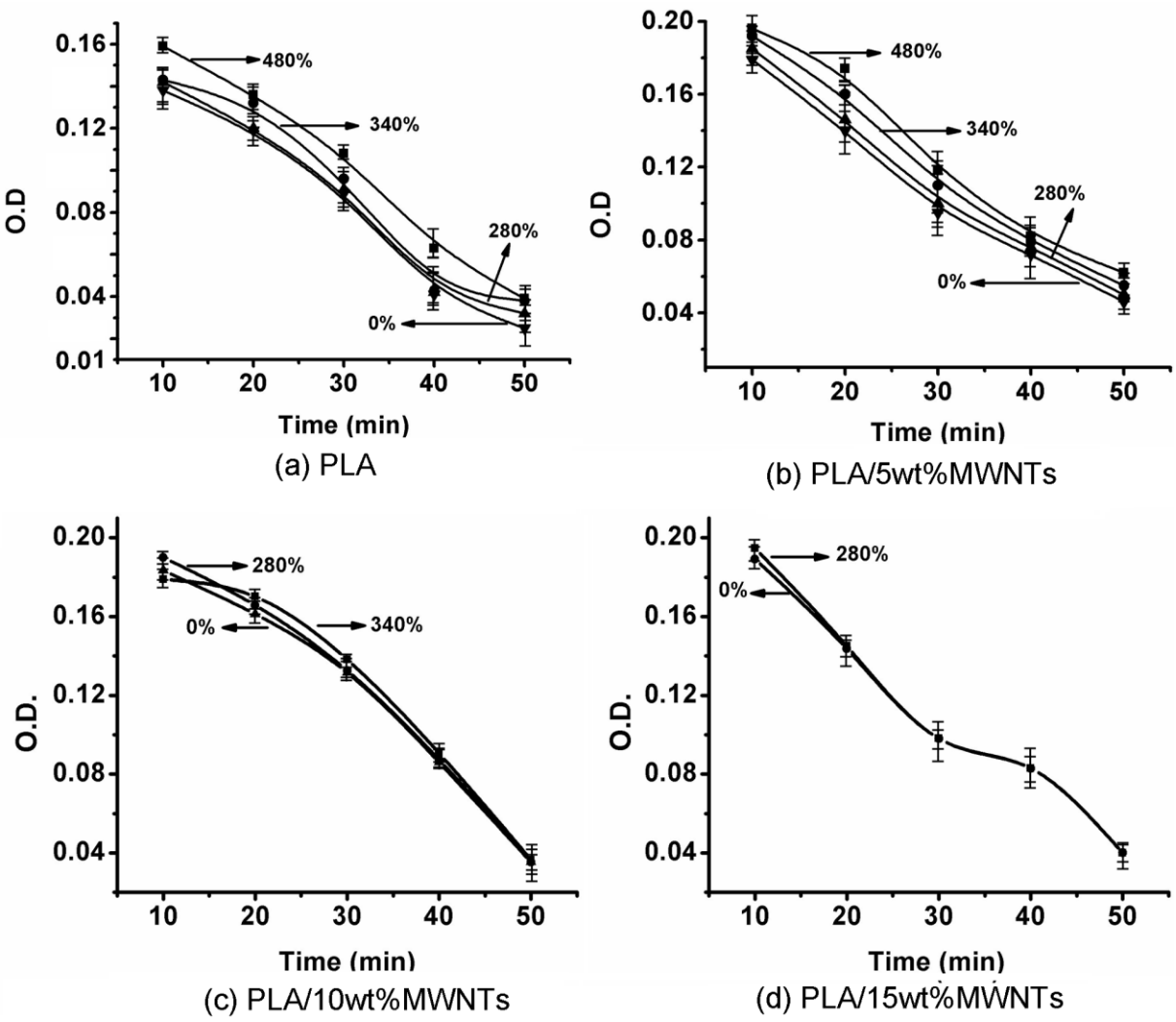

Figure 5 Curves of kinetic clotting time of oriented PLA and PLA/MWNTs composites

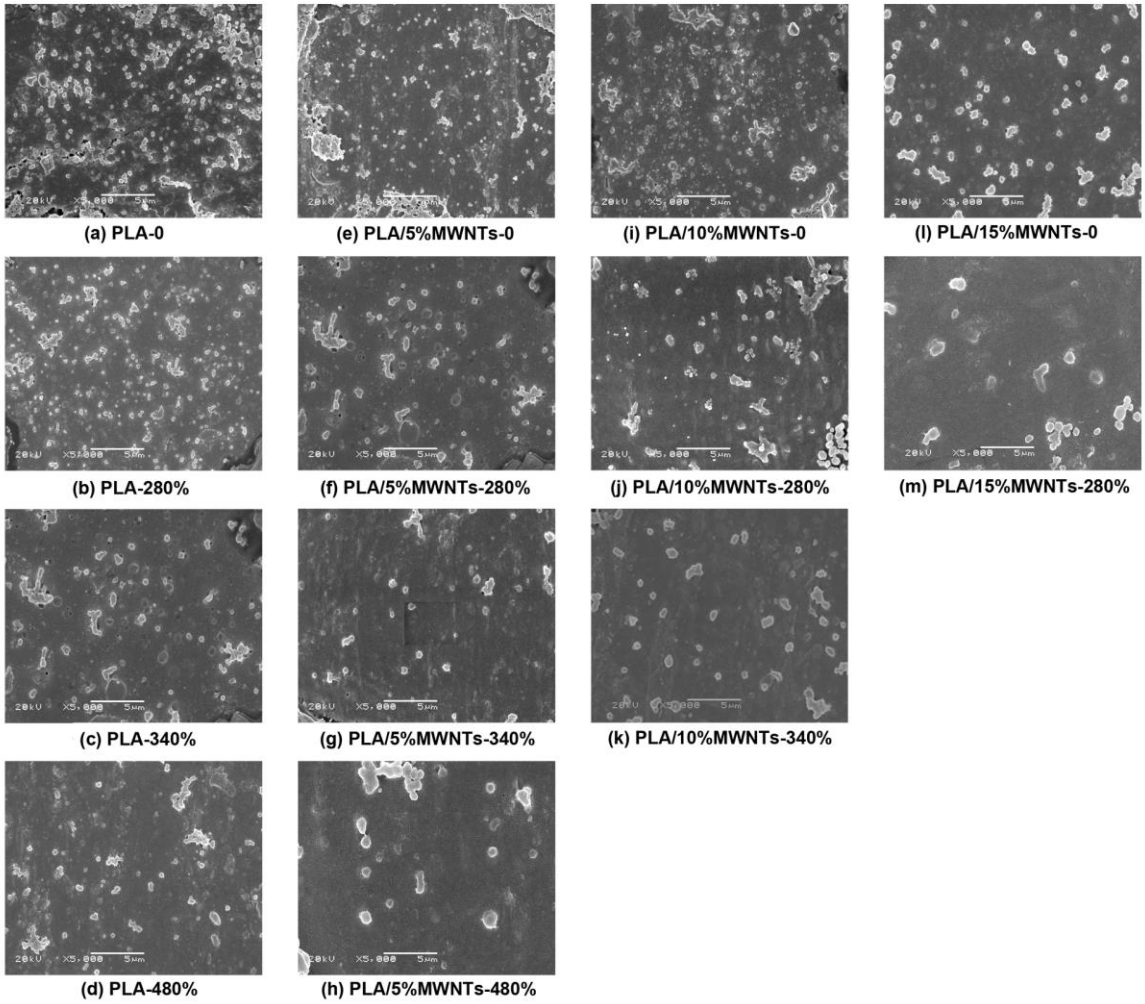

Figure 6 Platelet adsorption of oriented PLA and PLA/MWNTs composites（Magnification: 5000×）